Photosystem II Photoinactivation, Repair, and Protection in Marine Centric Diatoms[1][OA]

Hongyan Wu, Suzanne Roy, Meriem Alami, Beverley R. Green, and Douglas A. Campbell*

Biology, Mount Allison University, Sackville, New Brunswick, Canada E4L 1G7 (H.W., D.A.C.); College of Biological Engineering, Hubei University of Technology, Wuhan, Hubei 430068, China (H.W.); Institut des sciences de la mer de Rimouski, Université du Québec, Rimouski, Quebec, Canada G5L 3A1 (S.R.); and Botany, University of British Columbia, Vancouver, British Columbia, Canada V6T 1Z4 (M.A., B.R.G.)

Diatoms are important contributors to aquatic primary production, and can dominate phytoplankton communities under variable light regimes. We grew two marine diatoms, the small *Thalassiosira pseudonana* and the large *Coscinodiscus radiatus*, across a range of temperatures and treated them with a light challenge to understand their exploitation of variable light environments. In the smaller *T. pseudonana*, photosystem II (PSII) photoinactivation outran the clearance of PSII protein subunits, particularly in cells grown at sub- or supraoptimal temperatures. In turn the absorption cross section serving PSII photochemistry was down-regulated in *T. pseudonana* through induction of a sustained phase of nonphotochemical quenching that relaxed only slowly over 30 min of subsequent low-light incubation. In contrast, in the larger diatom *C. radiatus*, PSII subunit turnover was sufficient to counteract a lower intrinsic susceptibility to photoinactivation, and *C. radiatus* thus did not need to induce sustained nonphotochemical quenching under the high-light treatment. *T. pseudonana* thus incurs an opportunity cost of sustained photosynthetic down-regulation after the end of an upward light shift, whereas the larger *C. radiatus* can maintain a balanced PSII repair cycle under comparable conditions.

Diatoms (Bacillariophyceae) are a major group of microalgae ubiquitous in all marine and freshwater ecosystems. They contribute about 40% of aquatic primary production and are thus central to biogeochemical cycling (Field et al., 1998; Strzepek and Harrison, 2004). Diatoms tend to dominate ecosystems characterized by highly mixed water bodies, where they have to cope with rapid changes in the underwater light climate. Depending on the rate of water mixing and depth of the upper mixed layer, diatoms can be exposed to episodic excess light, generating stressful conditions that impair photosynthesis through photoinactivation, down-regulation, or oxidative stress (Long et al., 1994; Lavaud, 2007; Dubinsky and Stambler, 2009; Janknegt et al., 2009).

To cope with the potentially damaging effects of light, and to maintain photosynthesis, diatoms, like all oxygenic photoautotrophs, must counter the photoinactivation of PSII with repair through proteolytic removal of photodamaged proteins (Silva et al., 2003; Nixon et al., 2010) and the coordinated insertion of newly synthesized subunits into the thylakoid membrane (Aro et al., 1993; Komenda et al., 2012). If photoinactivation outruns the rate of repair, the PSII pool suffers net photoinhibition (Aro et al., 2005; Nishiyama et al., 2005, 2006; Murata et al., 2007), leading ultimately to a decrease in photosynthetic quantum yield and/or capacity. In comparison with other marine phytoplankton groups, including cyanobacteria and prasinophyte green algae (Six et al., 2007, 2009), diatoms show a lower susceptibility to primary photoinactivation (Key et al., 2010), and also distinctive clearance patterns for the PsbA (D1), PsbD (D2), and PsbB (CP47) PSII subunits upon an increase in light, in comparison with most other taxa examined to date (Wu et al., 2011). Intriguingly, the diatom chloroplasts have thylakoids arranged in a triple layer without distinct grana stacked regions (Lepetit et al., 2012), suggesting that distinct aspects of the diatom PSII repair cycle may relate to structural differences between chloroplasts with chlorophyll *a*/*c* light-harvesting antenna and those with chlorophyll *a*/*b* antenna, where the grana stacks impose spatial and temporal organization upon PSII repair (Aro et al., 1993, 2005; Nixon et al., 2010).

Upon a sudden increase in irradiance, another important short-term process for the photoprotection of PSII is the nonradiative dissipation of excess energy

[1] This work was supported by the Natural Sciences and Engineering Research Council of Canada (to D.A.C., B.R.G., S.R.) and the Canada Foundation for Innovation (to D.A.C.); the National Basic Research Program of China (grant nos. 2009CBA421207 and 2011CB200902); and the National Natural Science Key Foundation of China (grant no. 40930846 to H.W.). AgriSera AB and Environmental Proteomics kindly donated antibodies and protein quantitation standards.

* Corresponding author; e-mail dcampbell@mta.ca.

The author responsible for distribution of materials integral to the findings presented in this article in accordance with the policy described in the Instructions for Authors (www.plantphysiol.org) is: Douglas A. Campbell (dcampbell@mta.ca).

[OA] Open Access articles can be viewed online without a subscription.

www.plantphysiol.org/cgi/doi/10.1104/pp.112.203067

(Müller et al., 2001). Diatoms can dissipate excess light energy through distinct mechanisms of nonphotochemical quenching (NPQ) to limit overexcitation of their photosystems (Lavaud et al., 2002a, 2002b, 2004; Eisenstadt et al., 2008; Grouneva et al., 2008, 2009; Bailleul et al., 2010; Zhu and Green, 2010; Depauw et al., 2012; Lepetit et al., 2012).

Some NPQ mechanisms are associated with the operation of a xanthophyll cycle, which converts epoxidized to deepoxidized forms of certain xanthophylls. The carotenoid pigments in diatoms include fucoxanthin, β,β-carotene, and the xanthophyll-cycle pigment diadinoxanthin (Dd), which can be deepoxidized to form diatoxanthin (Dt). A pH gradient across the thylakoid membrane mediates NPQ formation (Lavaud and Kroth, 2006). Diatom NPQ can be linearly related to the Dt content (Lavaud et al., 2002a, 2002b, 2004, 2007), but species and ecotypes vary in their induction of NPQ (Lavaud et al., 2004; Schumann et al., 2007; Bailleul et al., 2010). Recently, Bailleul et al. (2010) and Zhu and Green (2010) showed evidence that the magnitude of NPQ induction is correlated with the expression level of Lhcx members of the chlorophyll *a*/*c* light-harvesting protein family.

The ability of diatoms to grow and dominate in light environments with large fluctuations in irradiance suggests an unusual photosynthetic flexibility, especially in harvesting, using or dissipating (Janknegt et al., 2009; Waring et al., 2010) variable levels of light energy over short time scales. Diatom growth and metabolism is also affected by temperature (Anderson, 2000), and the surface temperature of ocean waters is now expected to rise by 1°C to 7°C by 2100 (Houghton et al., 2001). Such an increase in temperature might influence diatom dominance of variable environments by modifying diatom responses to sudden increases in irradiance. We earlier showed that the primary susceptibility to the photoinactivation of PSII is inversely proportional to cell volume in diatoms (Key et al., 2010), so small and large diatoms have different balances between light-dependent photoinactivation and the counteracting temperature-dependent metabolic repair of PSII. We therefore quantitatively analyzed PSII photoinactivation, subunit turnover, pigment dynamics, and the kinetics of NPQ formation in two marine-centric diatoms, the small *Thalassiosira pseudonana* and the large *Coscinodiscus radiatus*, cultured under different temperatures and treated with a light challenge, to understand how PSII photoinactivation and repair, pigment dynamics, and Lhcx isoforms interact to generate the strong diatom capacity to exploit variable light.

RESULTS

Photoinhibition of the Photochemical Yield of PSII

T. pseudonana and *C. radiatus* cells were grown at different temperatures under 30 μmol photons m^{-2} s^{-1}, a light level approximating the bottom 10% of the photic zone. To assess their capacity to exploit variable light, we challenged them with a 90-min shift to 450 μmol blue photons m^{-2} s^{-1}, approximating a rapid mixing up to the light field in the upper third of the photic zone. After the light challenge, cells were shifted back to their original low growth light to track recovery and relaxation processes.

We used a multiple-turnover saturating flash and modulated fluorometer to estimate the maximum photochemical yield of PSII using the F_V/F_M ratio. In the smaller species *T. pseudonana* (cell volume of 19 ± 0.6 μm^3), F_V/F_M was 0.66 ± 0.005 for cells growing at 12°C, and 0.67 ± 0.01 for cells growing at 18°C or 24°C. In *T. pseudonana* cells maintaining a PSII repair cycle, F_V/F_M dropped significantly ($P < 0.05$) during the 90-min high-light exposure, but recovered ($P < 0.05$) during the subsequent growth light period regardless of the growth temperatures (Fig. 1, A–C). Compared with cells growing at 18°C, the sub- and supraoptimal growth temperatures of 12°C and 24°C led to significantly larger declines ($P < 0.05$) in F_V/F_M over 30 to 60 min before stabilizing late in the high-light treatment. Blocking the PSII repair cycle by adding lincomycin resulted in significant declines ($P < 0.05$) in F_V/F_M at all growth temperatures, with the loss of PSII activity following a single-phase exponential decay. In contrast, in the larger species *C. radiatus* (cell volume of 138,000 ± 6,150 μm^3) the maximum photochemical yield of PSII as measured by F_V/F_M ratio was 0.81 ± 0.003 for cells growing at 18°C, and 0.79 ± 0.01 for cells growing at 24°C. *C. radiatus* also showed lower susceptibility to high-light treatments, with smaller, although still significant ($P < 0.05$), decreases in F_V/F_M in the cells treated without or with lincomycin at both 18°C and 24°C (Fig. 1, D and E).

Turnover of PSII Subunits

We quantified the levels and variation in the content of key PSII proteins PsbA and PsbD during the 90-min high-light exposure and the subsequent 30-min recovery, for cells grown across a range of temperatures. *T. pseudonana* showed no significant change in total PsbA content in the control cells with active PSII repair cycles (Fig. 2, A–C), but lincomycin-treated cells suffered a progressive, significant drop in PsbA to about 75% of time 0 levels by the end of the 90-min high-light treatment ($P < 0.05$ at all temperatures). Similarly, high-light treatment did not cause any net loss of PsbA in the control cells of *C. radiatus*, but lincomycin-treated cells showed a significant net decline in PsbA content (Fig. 2, D and E; $P < 0.05$ at both temperatures).

In *T. pseudonana* cells with an active PSII repair cycle, PsbD varied but did not show significant change in cells grown at 12°C (Fig. 3A), declined somewhat in those grown at 18°C ($P < 0.05$; Fig. 3B), or remained nearly steady in those grown at 24°C (Fig. 3C). At all temperatures *T. pseudonana* cells treated with lincomycin showed a significant decline in PsbD ($P < 0.05$), which did not recover during the subsequent 30 min at

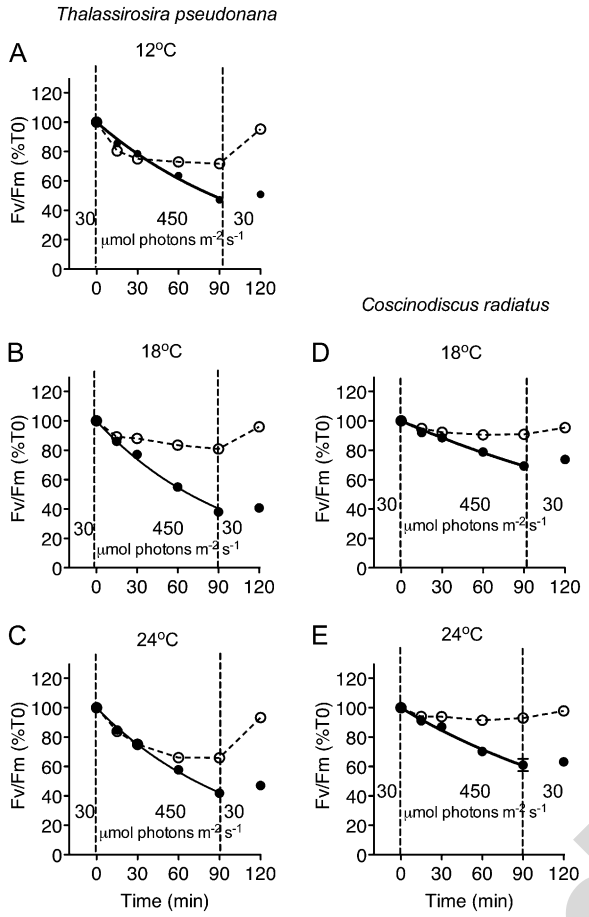

Figure 1. Responses of PSII maximum photochemical yield (F_V/F_M) versus time in *T. pseudonana* (A–C) and *C. radiatus* (D and E) cultures treated with (closed symbols) or without (open symbols) the chloroplast protein synthesis inhibitor lincomycin. Bothspecies were grown at 30 μmol photons m^{-2} s^{-1} at 12°C (A), 18°C (B and D), or 24°C (C and E), then exposed to 450 μmol photons m^{-2} s^{-1} blue light for 90 min, and then allowed to recover at 30 μmol photons m^{-2} s^{-1} for 30 min. n = 4 to 5 independent culture experiments, ±SE; most error bars within symbols.

lower light (Fig. 3, A–C). *C. radiatus* showed a significant accumulation of PsbD content upon a shift to high light ($P < 0.05$), which was blocked by the addition of lincomycin both at 18°C and 24°C (Fig. 3, D and E). Overall, the changes in the pools of PsbA and PsbD show significant departures in magnitude and even in direction from the patterns of PSII activity shown in Figure 1.

In Figure 4 we plot the first-order rate constants for removal of PsbA versus the rate constant for photoinactivation of PSII, for cells treated with lincomycin to block counteracting repair processes. In *T. pseudonana* photoinactivation consistently outruns the removal of PsbA. In *C. radiatus* the rate constants for removal of PsbA nearly meet the slower rate constants for photoinactivation of PSII. Both diatoms show a saturation profile for the rate constant for removal of PsbA, which reaches a maximum of about $8 \times 10^{-5} \pm 2 \times 10^{-5}$ s^{-1} (estimated using a Michaelis-Menten fit of the data with an overall R^2 of 0.45), even though photoinactivation can be much faster under high-light treatments. The rate constant estimates for treatments under red and white light are derived from data originally published in Wu et al. (2011).

Changes in Pigmentation

The major pigments in *T. pseudonana* and *C. radiatus* are chlorophyll *a*, chlorophyll c_2, fucoxanthin, diadinoxanthin (Dd), diatoxanthin (Dt), and β,β-carotene. Growth temperature did not cause large changes in the pigment content in either species under the low growth light level of 30 μmol m^{-2} s^{-1} (Table I). The levels of chlorophyll *a*, chlorophyll c_2, fucoxanthin, and β,β-carotene were steady throughout the high-light shift and the subsequent recovery periods in both species, both in the absence and the presence of lincomycin (data not shown), so our cultures neither lost

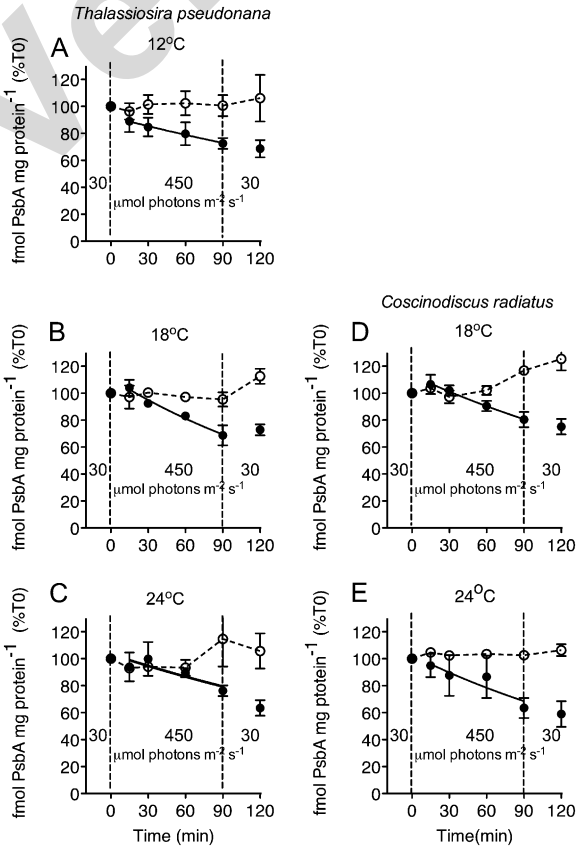

Figure 2. Changes in PsbA content in *T. pseudonana* (A–C) and *C. radiatus* (D and E) cultures treated with (closed symbols) or without (open symbols) the chloroplast protein synthesis inhibitor lincomycin. Both species were grown at 30 μmol photons m^{-2} s^{-1} at 12°C (A), 18°C (B and D), or 24°C (C and E), then exposed to 450 μmol photons m^{-2} s^{-1} blue light for 90 min, and then allowed to recover at 30 μmol photons m^{-2} s^{-1} for 30 min. n = 3, ±SE.

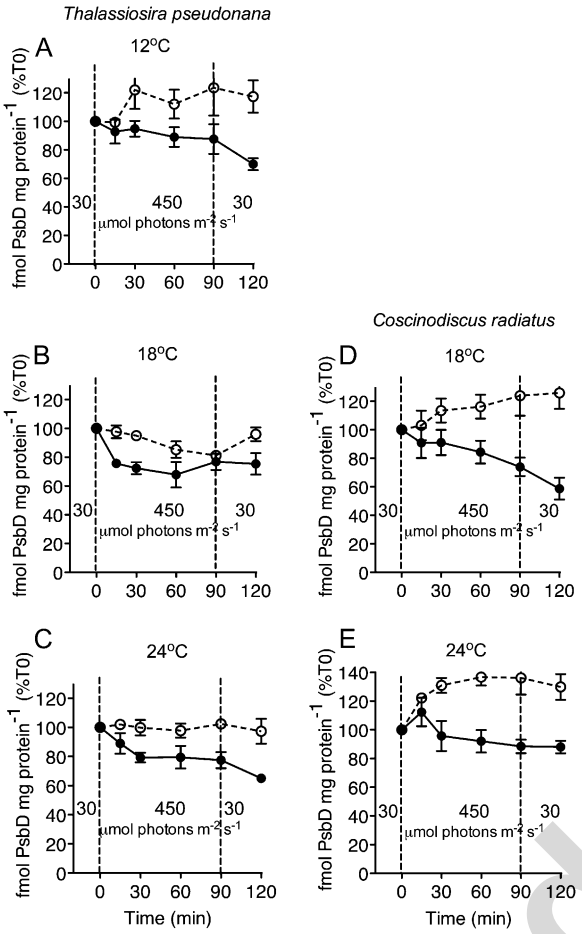

Figure 3. Changes in PsbD content in *T. pseudonana* (A–C) and *C. radiatus* (D and E) cultures treated with (closed symbols) or without (open symbols) the chloroplast protein synthesis inhibitor lincomycin. Both species were grown at 30 μmol photons m^{-2} s^{-1} at 12°C (A), 18°C (B and D), or 24°C (C and E), then exposed to 450 μmol photons m^{-2} s^{-1} blue light for 90 min, and then allowed to recover at 30 μmol photons m^{-2} s^{-1} for 30 min. $n = 3$, ±SE.

nor accumulated net light-harvesting pigments during our short high-light treatments.

In *T. pseudonana*, Dd was rapidly deepoxidized to Dt when cells were shifted to higher light (Fig. 5, A–C; $P < 0.05$), particularly in cells at 12°C and 24°C. Our earliest pigment time point was at 15 min, but in similar treatments Zhu and Green (2010) found that this conversion of Dd to Dt was largely complete within 2 min of high-light treatment. When cultures were shifted to low growth light for recovery, Dt was epoxidized back to Dd within 30 min ($P < 0.05$), and perhaps sooner. The pool size of Dd + Dt increased ($P < 0.05$) in all *T. pseudonana* cultures in the presence and absence of lincomycin, but deepoxidation of Dt was partially inhibited in cultures treated with lincomycin (data not shown; Bachmann et al., 2004). For *C. radiatus* the pool size of Dd + Dt increased ($P < 0.05$), indicating de novo synthesis, but the cells showed only slight, although statistically significant ($P < 0.05$) accumulations of Dt, much smaller than for *T. pseudonana* (Fig. 5, D and E).

NPQ Induction and PSII Functional Absorption Cross Section

Diatoms have significant capacities to induce different phases of NPQ, which lower the achieved photochemical yield of PSII. Figure 6 shows the dynamic NPQ_d phase, which relaxes within 5 min of dark incubation and is reinduced during a brief exposure to the treatment light; the sustained NPQ_s phase that persists beyond 5 min of dark incubation, and the total $NPQ_t = NPQ_d + NPQ_s$. In *T. pseudonana* cells with an active PSII repair cycle, those grown and treated at 12°C and 24°C showed a decrease in NPQ_d across the period of high-light exposure, but with a mirror increase in NPQ_s (Fig. 6, A–C). This shift from NPQ_d to NPQ_s reversed during the low-light recovery period. In *T. pseudonana* cells growing at their optimal temperature of 18°C NPQ_d was steady and there was only a limited, though significant ($P < 0.05$) accumulation of NPQ_s over the 90-min high-light treatment. For both *T. pseudonana* and *C. radiatus*, NPQ_s accumulated and subsequently relaxed even when chloroplastic protein synthesis was blocked by lincomycin (data not shown). In *T. pseudonana* the total NPQ_t was highest in cells grown at 12°C, and increased significantly ($P < 0.05$) during the high-light treatment. In *C. radiatus* (Fig. 6, D and E) the level of NPQ_t was much lower and there was only a slight accumulation of NPQ_s that did not

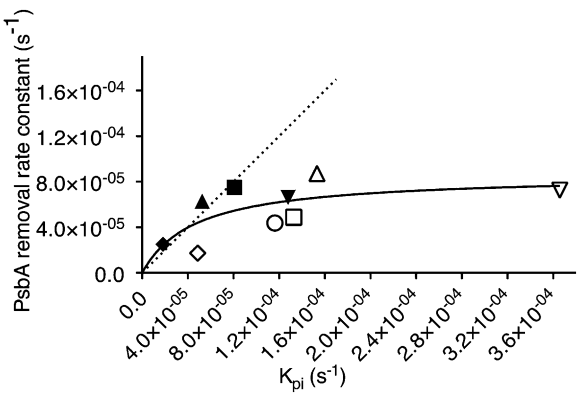

Figure 4. Correlation of PsbA removal rate constant (s^{-1}) and photoinactivation rate constant of PSII (k_{pi}, s^{-1}) in *T. pseudonana* cells grown at 30 μmol photons m^{-2} s^{-1}, 12°C (open circle), 18°C (open upward triangle, diamond, downward triangle), or 24°C (open square) and *C. radiatus* cells grown at 18°C (closed upward triangle, diamond, downward triangle) or 24°C (closed square). Rate constants were estimated from samples taken during 90 min of exposure to 450 μmol photons m^{-2} s^{-1} blue light (circles, upward triangles, squares) or 450 μmol photons m^{-2} s^{-1} red light (diamonds), or 1,400 μmol photons m^{-2} s^{-1} white fluorescent light (downward triangles). $n = 3$ to 5, ±SE for both *x* and *y* axes. Dotted line indicates 1:1 ratio; solid line shows a hyperbolic tangent Michaelis-Menten curve fit to the data, showing saturation of the PsbA removal rate constant.

Table I. *Growth rate, PSII reaction center protein, and pigment content of T. pseudonana and C. radiatus cells cultured at different temperatures and 30 μmol photons m^{-2} s^{-1}*

n = 3 to 5, ± SE.

Parameter	*T. pseudonana*			*C. radiatus*	
	12°C	18°C	24°C	18°C	24°C
μ (d^{-1})	0.8 (±0.01)	1.1 (±0.01)	1 (±0.01)	0.4 (±0.01)	0.4 (±0.01)
Proteins(fmol μg $protein^{-1}$)					
PsbA	51 (±7)	71 (±14.5)	67 (±5)	23 (±4)	30 (±4)
PsbD	137 (±10)	139 (±5)	163 (±33)	23 (±4)	16 (±1)
Chlorophyll *a* (fmol $cell^{-1}$)	0.3 (0.01)	0.3 (0.01)	0.3 (0.01)	254 (23)	299 (7)
Pigments (mol 100 mol Chl a^{-1})					
Fucoxanthin: Chl *a*	48 (±1)	53 (±0.5)	55 (±0.3)	61 (±1)	63 (±1)
β,β-Carotene: Chl *a*	5 (±1)	5 (±1)	5 (±1)	5 (±0.3)	5 (±0.4)
Dd: Chl *a*	12 (±0.4)	10 (±0.2)	11 (±0.3)	7 (±0.1)	8 (±0.2)

reach the threshold of statistical significance during the high-light treatment. Because our experiments involved short-term light-shift experiments to track PSII photoinactivation, we did not apply longer-term relaxation periods to estimate q_E and q_I according to Farber et al. (1997), as done by Zhu and Green (2010), although we have the 30-min low-light incubation at the end of the treatments, to track final relaxation of q_E and q_I phases.

Dark-adapted cells of the smaller species *T. pseudonana* had a larger functional absorption cross section serving PSII photochemistry (σ_{PSII}) than did the larger cells of *C. radiatus* (compare Fig. 7, A–C to D and E; species difference significant at $P < 0.05$ in a Bonferroni posttest after one-way ANOVA), consistent with pigment packaging or self-screening effects in the larger cells (Morel and Bricaud, 1981; Finkel, 2001; Key et al., 2010). In *T. pseudonana* there was a weak influence of growth temperature on σ_{PSII}, with cells growing at 12°C showing a σ_{PSII} of 250 A^2 $quanta^{-1}$, whereas cells growing at 18°C or 24°C showed a slightly larger σ_{PSII} of 260 A^2 $quanta^{-1}$ (temperature difference significant at $P = 0.05$ in a Bonferroni posttest after one-way ANOVA). *C. radiatus* did not show a significant effect of growth temperature on σ_{PSII}. These σ_{PSII} estimates for dark-adapted cells are very close to the σ_{PSII}' estimated for cells measured under their low growth light (data not presented). For *T. pseudonana* with an active PSII repair cycle, σ_{PSII} decreased slightly at all temperatures during the 90-min high-light treatment, but recovered to close to initial values after 30 min of recovery (Fig. 7, A–C). In *T. pseudonana* cells incubated with lincomycin to block the PsbA repair cycle, σ_{PSII} increased 20% as the cells suffered approximately 50% to 60% photoinhibition of PSII (compare Fig. 7, A–C with Fig. 1, A–C). When the functional absorption cross section of PSII was measured under the treatment light level of 450 μmol blue photons m^{-2} s^{-1}, σ_{PSII}' decreased to half the value of σ_{PSII} from dark-acclimated cells, consistent with the induction of NPQ_t by the treatment light (Fig. 6; significant at $P < 0.05$ using a Bonferroni posttest after one-way ANOVA). In contrast, σ_{PSII} was stable across the light-shift treatments in *C. radiatus* cells with or without lincomycin at both temperatures, and there was no significant down-regulation of σ_{PSII}' measured under the treatment light level of 450 μmol blue photons m^{-2} s^{-1}, in comparison to the σ_{PSII} measured from dark-acclimated cells (Fig. 7, D and E).

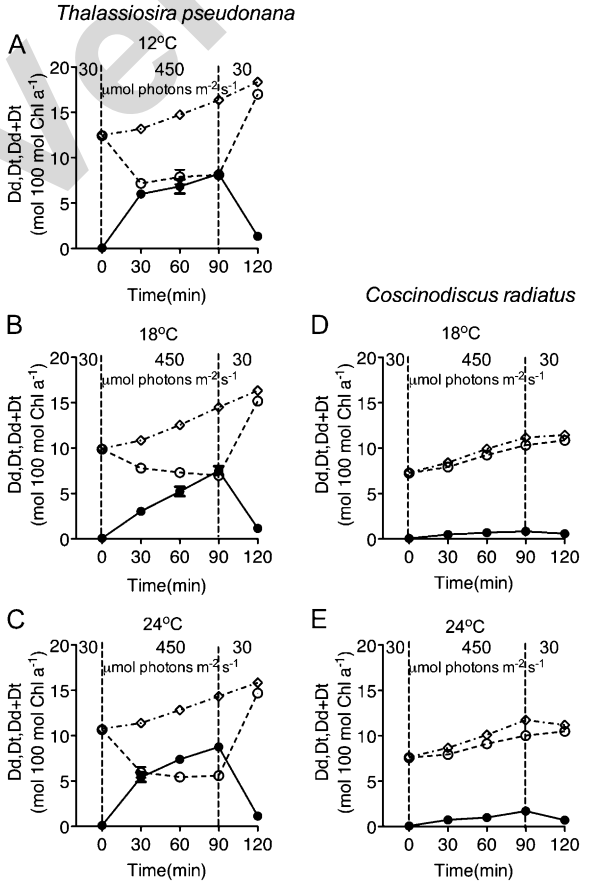

Figure 5. Dd and Dt kinetics in *T. pseudonana* (A–C) and *C. radiatus* (D and E) cultures with active PSII repair. Dd (open circles), Dt (closed circles), and Dd + Dt (open diamonds) were measured with cells that were grown at 30 μmol photons m^{-2} s^{-1} at 12°C (A), 18°C (B and D), or 24°C (C and E), then exposed to 450 μmol photons m^{-2} s^{-1} blue light for 90 min, and then allowed to recover at 30 μmol photons m^{-2} s^{-1} for 30 min. $n = 3$, ±SE.

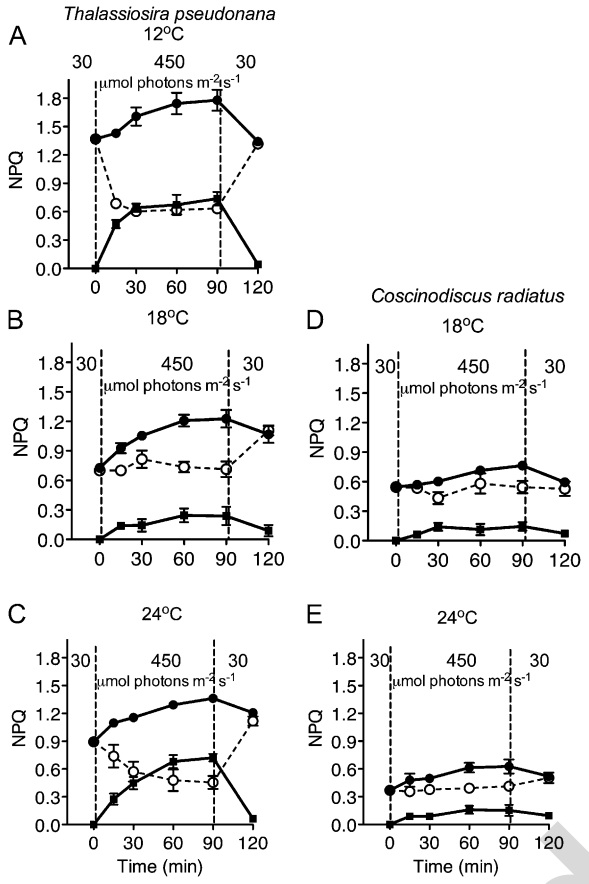

Figure 6. Responses of rapidly reversible, dynamic NPQ (open circles; $NPQ_d = [F_M - F_M']/F_M'$); sustained NPQ (closed squares; $NPQ_s = [F_{Mt0} - F_M]/F_M$), and total NPQ (closed circles; $NPQ_t = NPQ_s + NPQ_d$) versus time in *T. pseudonana* (A–C) and *C. radiatus* (D and E) cultures with active PSII repair. Both species were grown at 30 μmol photons m^{-2} s^{-1} at 12°C (A),18°C (B and D), and 24°C (C and E), then exposed to 450 μmol photons m^{-2} s^{-1} blue light for 90 min, and then allowed to recover at 30 μmol photons m^{-2} s^{-1} for 30 min. n = 4 to 5 separate culture experiments, ±SE.

In *T. pseudonana*, NPQ_s was significantly correlated with the deepoxidation state (DES) of the xanthophyll cycle pigments, calculated as DES = Dt/(Dd + Dt) (Fig. 8B; F test for slopes nonzero at $P < 0.015$ for cells growing at 12°C, 18°C, and 24°C; R^2 for regression lines 0.98 at 12°C, 0.89 at 18°C, and 0.99 at 24°C). *T. pseudonana* cells grown at 12°C and 24°C, however, induced much more NPQ_s at a given DES level than did cells at the optimal growth temperature of 18°C (slopes at 12°C and 24°C significantly higher than at 18°C, $P < 0.0001$). In *C. radiatus* DES remained low (Fig. 5, D and E) across the light treatment, as did NPQ_s (Fig. 6, D and E) so we did not plot regressions of these data.

T. pseudonana showed significant temperature and light induction patterns for the Lhcx1 (Fig. 9A) and Lhcx6 (Fig. 9B) chlorophyll proteins. Lhcx1 levels were markedly higher ($P < 0.05$) in cells growing at 12°C than at 18°C or 24°C (Bonferroni posttests $P < 0.05$ after two-way ANOVA), but then increased further in cells shifted to higher light for 90 min under all three growth temperatures (Fig. 9A; Bonferroni posttests $P < 0.05$ after two-way ANOVA). In agreement with our previous work (Zhu and Green, 2010), Lhcx6 could not be detected under low light at 18°C, but was detected in cells grown at 12°C, suggesting a cold stress or excitation pressure (Huner et al., 1998) response (Fig. 9B). The high-light-induced increase was also stronger at lower temperature (Bonferroni posttests $P < 0.05$ after two-way ANOVA), again consistent with an excitation-pressure response. Since both the anti-Lhcx1 and anti-Lhcx6 antibodies were raised to gene-specific C-terminal peptides (Zhu and Green, 2010), we did not detect bands in total protein extracts from *C. radiatus* (data not presented). Under the same treatments, DES induction in *T. pseudonana* increased

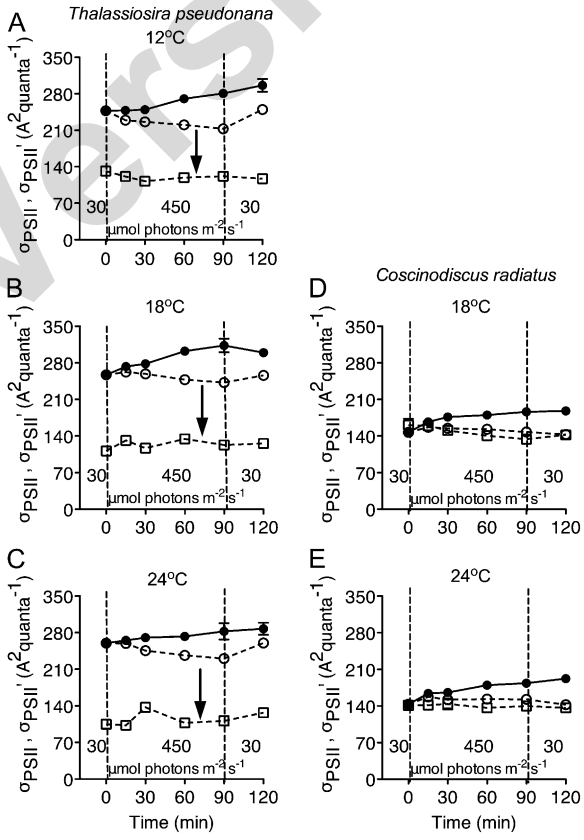

Figure 7. Changes in PSII effective absorption cross section (σ_{PSII}), estimated from flash fluorescence rise kinetics, in *T. pseudonana* (A–C) and *C. radiatus* (D and E) cultures treated with (closed symbols) or without (open symbols) the chloroplast protein synthesis inhibitor lincomycin. Both species were grown at 30 μmol photons m^{-2} s^{-1} at 12°C (A), 18°C (B and D), or 24°C (C and E), then exposed to 450 μmol photons m^{-2} s^{-1} blue light for 90 min, and then allowed to recover at 30 μmol photons m^{-2} s^{-1} for 30 min. Circles represent σ_{PSII} measured in the dark, squares represent σ_{PSII}' measured under the treatment light of 450 μmol photons m^{-2} s^{-1} blue light. n = 4 to 5 independent culture experiments, ±SE; most error bars within symbols. Downward arrows indicate light-driven down-regulation of σ_{PSII} to σ_{PSII}' in *T. pseudonana*.

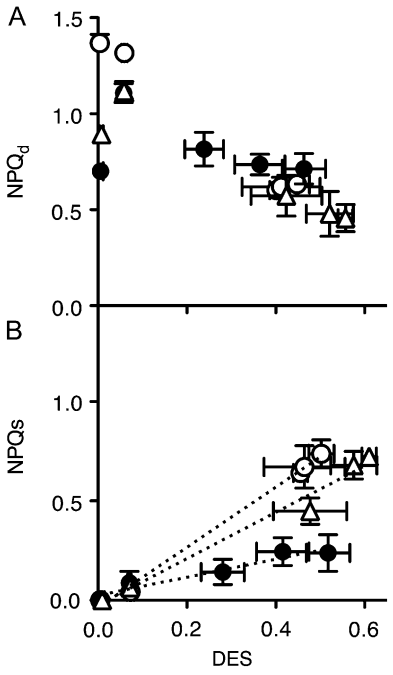

Figure 8. NPQ_d (A) and NPQ_s (B) versus DES, Dt/(Dd + Dt) in *T. pseudonana* cells grown at 12°C (open circles), 18°C (closed circles), or 24°C (open triangles) over 90 min of exposure to 450 μmol photons m^{-2} s^{-1} blue light. $n = 3$ to 5, ±SE.

with increasing temperature (Fig. 9C; two-way ANOVA with Bonferroni posttests $P < 0.05$). NPQ_t was lowest in cells growing at the optimal 18°C (Fig. 9D), although the upward light shift still provoked a significant increase in NPQ_t (two-way ANOVA with Bonferroni posttests $P < 0.05$).

Figure 10 summarizes these findings for the two species by showing that the accumulation of NPQ_s correlates (nonzero slope, $R^2 = 0.62$) with the ratio of the rate constants for photoinactivation of PSII and the removal of PsbA protein. When photoinactivation outruns removal of PsbA protein the diatoms induce NPQ_s. Data points from white-light and red-light treatments of *T. pseudonana* and *C. radiatus* are estimated from data originally published in Wu et al. (2011).

DISCUSSION

PSII Photoinactivation Can Outrun PSII Protein Turnover

Turnover of the PsbA protein is required for PSII repair and restoration of PSII photochemical activity after photoinactivation (Aro et al., 1993; Murata et al., 2007; Edelman and Mattoo, 2008; Nixon et al., 2010; Komenda et al., 2012), but PSII repair is a separate, multistep process that shows kinetic departures from PSII photoinactivation (Edelman and Mattoo, 2008). Both *T. pseudonana* and *C. radiatus* were able to maintain or increase their total pools of PsbA and PsbD proteins when the repair cycle was active (Figs. 2, A–C and 3, A–C), demonstrating active synthesis of the PsbA and PsbD proteins. In *T. pseudonana* at 18°C this maintenance of PsbA protein levels was consistent with nearly stable PSII quantum yields during the shift to higher light (Fig. 1B), similar to Zhu and Green (2010). *T. pseudonana* grown at 12°C and 24°C also maintained PsbA protein levels (Fig. 2, A and C) but the PSII quantum yield declined (Fig. 1, A and C) during the high-light exposure period, showing that maintenance of PsbA protein pools (Fig. 2, A and C)

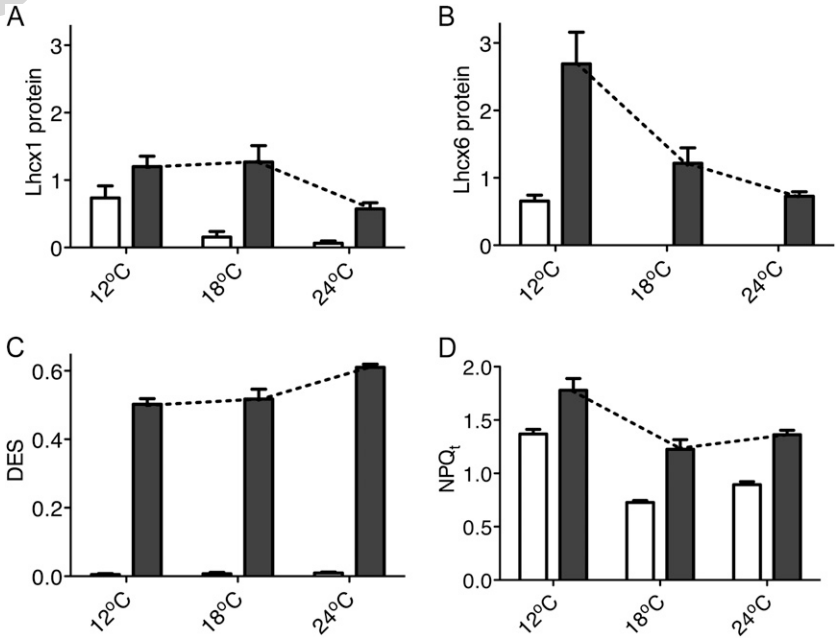

Figure 9. Lhcx1 protein (A), Lhcx6 protein (B), DES, Dt/(Dd + Dt) (C), NPQ_t (D) in *T. pseudonana* cells grown at 12°C, 18°C, or 24°C before (open bars) and after (closed bars) 90 min of exposure to 450 μmol photons m^{-2} s^{-1} blue light. $n = 3$ to 5, ±SE. Relative protein levels (A and B) detected by immunostaining were normalized to the 20-kD band of MagicMark XP marker (Invitrogen) run in parallel on each gel. Dotted lines emphasize the temperature pattern of inductions under high light.

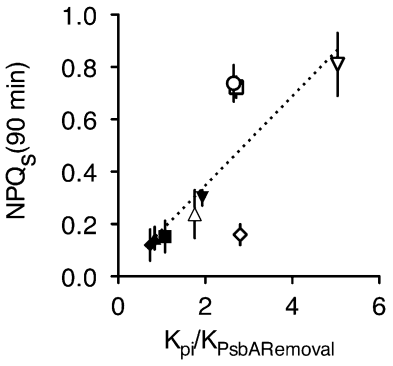

Figure 10. Sustained NPQ accumulates when PSII photoinactivation outruns repair. Accumulated NPQ_s plotted versus the ratio of the photoinactivation rate constant for PSII (k_{pi}) and the PsbA removal rate contant, for *T. pseudonana* cells grown at 30 μmol photons m^{-2} s^{-1}, 12°C (open circle), 18°C (open upward triangle, diamond, downward triangle), or 24°C (open square) and *C. radiatus* cells grown at 18°C (closed upward triangle, diamond, downward triangle) or 24°C (closed square). NPQs and rate constants were estimated from samples taken during 90 min of exposure to 450 μmol photons m^{-2} s^{-1} blue light (circles, upward triangles, squares) or 450 μmol photons m^{-2} s^{-1} red light (diamonds), or 1,400 μmol photons m^{-2} s^{-1} white fluorescent light (downward triangles). $n = 3$ to 5, ±SE for both x and y axes. Dotted line shows linear regression, $R^2 = 0.62$.

did not alone suffice for these cells to maintain their pool of active PSII, and that cells can accumulate subpools of PsbA and PsbD beyond their pools of active PSII.

When PSII repair is blocked in *T. pseudonana* the upward light shifts provoke photoinactivation of PSII (Fig. 1, A–C) that can outrun the clearance of PsbA protein (Figs. 2, A–C and 4). Edelman and Mattoo (2008) have reviewed similar data from other taxa showing that turnover of PsbA protein shows light saturation at moderate light, much different from photoinactivation rates that increase with increasing light. Conversely, in *T. pseudonana* elevated red light activates removal of PsbA that can outrun photoinactivation, at least transiently (Wu et al., 2011), showing that even under low light *T. pseudonana* can maintain pools of PSII repair cycle intermediates aside from the pool of active PSII. In *T. pseudonana* grown under low light the clearance of PsbA protein is light saturated at <450 μmol photons m^{-2} s^{-1} (Wu et al., 2011; H. Wu and D. Campbell, unpublished data), with a maximum rate constant of about 8×10^{-5} s^{-1} (Fig. 4). We initially anticipated that clearance of PsbA, as a process of protein metabolism, would show a positive correlation with growth temperature. In fact, the rate constant for removal of PsbA (Fig. 4) and the growth rate of *T. pseudonana* (Table I) both peaked at 18°C. Intriguingly, the growth rate of *T. pseudonana* is supersaturated by light at <450 μmol photons m^{-2} s^{-1} (G. Li and D. Campbell, unpublished data), suggesting that cells reach a mechanistic upper limit on their capacity to clear PsbA from photoinactivated PSII.

The larger, slower-growing cells of *C. radiatus* present a contrast since under the given light treatment *C. radiatus* suffers less photoinactivation, a manifestation of the negative size scaling of diatom susceptibility to photoinactivation (Key et al., 2010), which probably reflects light screening in larger cells (Finkel, 2001). Even though *C. radiatus* grows more slowly (Table I) it achieves rate constants for removal of PsbA similar to *T. pseudonana* (Figs. 2, D and E and 4), and thus PsbA removal can keep pace with the slower photoinactivation in *C. radiatus* (Fig. 4). We suspect that the saturation of the rate constant for removal of PsbA at around 8×10^{-5} s^{-1} (Fig. 4) reflects a fundamental property of the PSII repair cycle in these diatoms, with their triply stacked thylakoids and lack of apparent grana/stroma regions (Lepetit et al., 2010), rather than a size-dependent variable related to size scaling of growth rate or metabolic rate (Finkel, 2001). These differences in the balance between photoinactivation and PsbA and PsbD turnover in *T. pseudonana* and *C. radiatus* prove to have important consequences for the different induction patterns of NPQ and antenna function in the two species under comparable light treatments.

Antenna Function and Induction of NPQ

Algae can respond to sustained high light by changing the size of the PSII antenna by modifying the composition and the arrangement of pigments in relation to the PSII reaction center content, a strategy termed σ-type acclimation (Falkowski and Owens, 1980; Dubinsky and Stambler, 2009). In this study, except for the xanthophyll cycle pigments, neither species showed short-term changes in their contents of accessory pigments or chlorophyll *a* (data not shown), and the functional absorption cross sections (σ_{PSII} and σ_{PSII}') of the two species remained nearly stable during the 90-min high-light exposure (Fig. 7). For *T. pseudonana* cultures that suffered progressive loss of PSII function in the presence of lincomycin (Fig. 1, A–C, closed symbols), the σ_{PSII} of the remaining PSII centers showed a modest increase after the 90-min high-light exposure (Fig. 7,

Table II. *Definitions of chlorophyll fluorescence parameters*

Parameter	Equation	Similar Parameter	Reference
F_V/F_M	$(F_M - F_0)/F_M$		van Kooten and Snel (1990)
NPQ_d	$(F_M - F_M')/F_M'$	NPQ	Bilger and Bjorkman (1990)
NPQ_s	$(F_{Mt0} - F_M)/F_M$	q_Z	Nilkens et al. (2010)
NPQ_t	$NPQ_d + NPQ_s$		

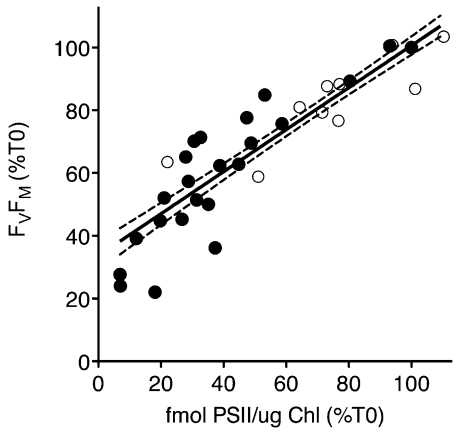

Figure 11. PSII maximum photochemical yield (F_V/F_M) correlates with content of functional PSII determined from oxygen evolution. *T. pseudonana* cultures were grown at 18°C under 30, 90, 180, or 270 μmol photons m^{-2} s^{-1} for many generations. We used a modulated fluorometer to measure F_V/F_M and an oxygen flash yield protocol to determine their content of active PSII. We then shifted the cultures to 90, 180, 270, 450, 1,000, 1,400, 1,800, or 2,200 μmol photons m^{-2} s^{-1} for 30 to 90 min, with or without lincomycin, and then remeasured F_V/F_M and active PSII content. open circles: cultures measured with active PSII repair; closed circles: cultures measured in the presence of the chloroplast translation inhibitor lincomycin to block PSII repair. Line shows the linear regression for the pooled data since an *F* test found no significant difference between the slopes for the data with or without lincomycin. R^2 = 0.89, dotted lines show 95% confidence interval for linear regression line. *y* intercept for pooled data = 33.6% ± 2.3%. Diatom PSII photoinactivation, repair, and protection.

A–C), consistent with limited connectivity across the antennae serving the active PSII centers (Mauzerall, 1982). In *T. pseudonana* σ_{PSII}' measured under the growth light of 30 μmol photons m^{-2} s^{-1} was very close to the σ_{PSII} measured in the dark (data not presented) while σ_{PSII}' measured under the treatment light level of 450 μmol photons m^{-2} s^{-1} dropped to half the size of σ_{PSII} measured in dark-acclimated cells (Fig. 7, A–C), showing strong short-term down-regulation of antenna function in the face of increasing light. The magnitude of this down-regulation is mirrored by light induction of NPQ (Fig. 6), which is mediated at least in part by the diatom xanthophyll cycle (Lavaud et al., 2002b; Goss and Jakob, 2010). In *C. radiatus* σ_{PSII}' remained much closer to σ_{PSII} (Fig. 7, D and E), consistent with very limited induction of NPQ_s and lower overall NPQ_t under our treatment conditions.

In *T. pseudonana* Dd deepoxidated rapidly to Dt when cells were shifted to high light, and the pool size of Dd + Dt increased significantly during the high-light exposure in both diatom species (Fig. 5). In diatoms one Dd pool representing 40% to 60% of the total has a very low turnover (Goericke and Welschmeyer, 1992), is not convertible into Dt (Lohr and Wilhelm, 2001; Lavaud et al., 2004; Fig. 5), and may contribute to structural stabilization of pigment-protein complexes (Pascal et al., 1998). The other diatom Dd pool, representing 50% to 60% of the total, has a much higher turnover (Goericke and Welschmeyer, 1992), is converted into Dt, and may also serve as the precursor for fucoxanthin synthesis (Goericke and Welschmeyer, 1992; Lohr and Wilhelm, 1999, 2001). In our study the net fucoxanthin content was stable across the higher-light treatment and the subsequent low-light recovery period. However, fast accumulation of Dt from the deepoxidation of Dd was clear in *T. pseudonana*, especially over the first 2 to 30 min of high-light exposure (Fig. 5; Zhu and Green, 2010). In *T. pseudonana* the deepoxidation of Dd to Dt (DES) was not correlated with the rapidly reversible NPQ_d (Fig. 8; Zhu and Green, 2010), but DES was linearly correlated with the extent of sustained NPQ_s (Fig. 8B) and with the total NPQ_t (Fig. 8C). Our NPQ_s phase is consistent with the q_I estimates of Zhu and Green (2010) and appears similar to the q_Z quenching recently defined by Nilkens et al. (2010), which correlated with deepoxidation of xanthophyll pigments in Arabidopsis (*Arabidopsis thaliana*).

Diatoms show complex regulation of NPQ (Lohr and Wilhelm, 1999; Lavaud et al., 2002a, 2002b, 2004; Goss et al., 2006; Dimier et al., 2007; Lavaud, 2007; Eisenstadt et al., 2008; Grouneva et al., 2008, 2009; Goss and Jakob, 2010; Lepetit et al., 2010, 2012). The differences among studies reflect physiological distinctions in the rates and magnitudes of induction and relaxation of NPQ phases across taxa (e.g. Fig. 6) or growth conditions (e.g. Fig. 8), but also differences in the experimental sequences and durations of light, dark, and low-light incubations (Goss et al., 2006; Zhu and Green, 2010).

The slope of the correlation between NPQ_s induction and DES varied with the growth temperature in *T. pseudonana* (Fig. 8B). For the same amount of DES, more NPQ_t was induced in cells at the suboptimal growth temperature of 12°C (Fig. 8C), with less induction of NPQ_t at the optimal growth temperature of 18°C. Cells at 24°C achieved higher DES (Fig. 8, B and C). Variations in the efficacy of quenching induction in response to Dt accumulation occur among species (Lavaud et al., 2004) and across different ecotypes of *Phaeodactylum tricornutum* (Bailleul et al., 2010). A lower quenching efficiency of Dt could result if the newly synthesized Dt pool is located in a lipid shield surrounding the fucoxanthin chlorophyll proteins and is not necessarily protein bound (Lepetit et al., 2010, 2012). In addition, studies by Eisenstadt et al. (2008, 2010) showed that changes in the functional organization of the diatom PSII reaction center under higher excess light could lead to the formation of NPQ independently of Dt.

Levels of members of the Lhcx pigment protein family are implicated in modulating the magnitude of induction of NPQ in diatoms. Zhu and Green (2010) showed that the expression of the Lhcx6 protein is associated with modulation of NPQ_s induction in *T. pseudonana*, and Bailleul et al. (2010) showed a correlation between NPQ_d and one of the Lhcx1 homologs in *P. tricornutum*. Therefore, diatoms possess

overlapping means to dissipate excessive light energy. In Figure 9 we show that *T. pseudonana* has significant levels of Lhcx1 and Lhcx6 proteins during growth at 12°C. These 12°C cultures also show the highest baseline levels of total NPQ_t (Fig. 8C). Within 90 min of an upward shift to 450 μmol photons m^{-2} s^{-1} *T. pseudonana* induced further expression of Lhcx1 and Lhcx6, with the magnitude of induction negatively correlated with growth temperature (Fig. 9, A and B), a pattern consistent with regulation of Lhcx1 and Lhcx6 by excitation pressure (Huner et al., 1998). The light induction of Lhcx1 and Lhcx6 coincides with the conversion of rapidly reversible NPQ_d to sustained NPQ_s. In contrast to the negative temperature correlation of Lhcx induction, induction of DES is highest at the highest growth temperature of 24°C. Overall, the differential inductions of Lhcx isoforms and xanthophyll deepoxidation mediate the highest accumulation of NPQ_t at 12°C, where *T. pseudonana* suffered the biggest gap between photoinactivation and clearance of PsbA protein (Figs. 4 and 10).

CONCLUSION

Small and large centric diatom species react differentially to a comparable increase in light intensity (Key et al., 2010; Wu et al., 2011; Figs. 1–3 and 5–7). Figure 10 summarizes our findings by plotting the accumulation of sustained NPQ_s versus the ratios of the rate constants for photoinactivation (k_{pi}) and for removal of PsbA protein. In the smaller *T. pseudonana* PSII photoinactivation outran removal of PsbA protein (Figs. 1, 3, 4, and 10), the cells induced strong expression of Lhcx1 and Lhcx6 proteins (Fig. 9), and deepoxidated their xanthophyll cycle pigments (Fig. 5) to induce a sustained NPQ_s phase of NPQ (Figs. 6 and 10, open symbols). *T. pseudonana* grown at sub- or supraoptimal temperatures showed yet more reliance on induction of NPQ_s, to cope with a less-effective PSII repair cycle with yet slower subunit clearance. The high level of sustained NPQ down-regulated the *T. pseudonana* functional absorption cross section for PSII photochemistry (Fig. 7), down-regulating PSII activity for up to 30 min during a subsequent downward light shift. The resulting opportunity cost of lost photosynthesis under variable light is large relative to the direct metabolic cost of PSII turnover and repair (Long et al., 1994; Raven, 2011).

In contrast, in the larger, slower growing *C. radiatus* removal of PsbA was sufficient to largely keep pace with a slower rate of PSII photoinactivation (Figs. 4 and 10; Key et al., 2010; Wu et al., 2011). Under these conditions the larger *C. radiatus* could exploit the increase in light with little induction of NPQ_s (Figs. 6, D and E and 10, closed symbols) and thus without significant down-regulation of their functional absorption cross section for PSII photochemistry (Fig. 7). *C. radiatus* thus does not incur the opportunity cost of lost photosynthesis during a subsequent downward shift in light, pointing to a competitive advantage for the larger species under fluctuating light regimes (Lavaud et al., 2007).

MATERIALS AND METHODS

Culture Conditions and Growth Rates Calculation

The diatoms *Thalassiosira pseudonana* National Center for Marine Algae and Microbiota (NCMA, formerly CCMP) 1014 and *Coscinodiscus radiatus* NCMA 312 (both obtained from Provasoli-Guillard National Center for Marine Algae and Microbiota) were grown in semicontinuous batch cultures using K medium (Keller et al., 1987) in polystyrene flasks (Corning) at 12°C (for *T. pseudonana* only), 18°C, or 24°C. Cultures were grown under continuous light of 30 μmol photons m^{-2} s^{-1} provided by fluorescent tubes (Sylvania) and measured in the culture flasks using a microspherical quantum sensor (US-SQS; Walz) connected to a Li-Cor light meter (LI-250; Li-Cor). The cultures were agitated manually twice daily. Cell densities were monitored by cell counts using a Beckman counter (Multisizer 3) for *T. pseudonana* NCMA 1014. The cell counter also provides an equivalent spherical volume estimate for the counted cells. We used a Sedgwick-Rafter counting chamber under a light microscope to count *C. radiatus* NCMA 312, and estimated the cell volume by approximating the cells as cylinders, and measuring radius and cylinder height. Growth rate (μ) was estimated as

$$\mu = (\ln(N_t) - \ln(N))/t$$

where N_t is the number of cells at time t and N is the number of cells at time 0. All cultures were grown through at least four transfers of semicontinuous dilution with fresh media under the given light level, and went through more than 24 generations under the given light level to ensure full acclimation before use in subsequent experiments.

Upward Light Shift and Recovery Experiment

Culture replicates from exponential growth phase were split into two flasks, with 500 μg mL^{-1} lincomycin added to one flask to block chloroplast protein synthesis (Bachmann et al., 2004), thereby inhibiting PSII repair (Baroli and Melis, 1996; Tyystjärvi and Aro, 1996; Key et al., 2010). Both flasks were incubated in the dark for 10 min to allow the lincomycin to exert its effect and then exposed to broad-band blue light (LEE filter no. 183; 455- to 479-nm peak transmission, 406- to 529-nm half-height width) of 450 μmol photons m^{-2} s^{-1} for 90 min. This blue-light treatment was chosen to approximate a marine light-field quality, and to match the spectral band for our determinations of the functional absorption cross section serving PSII photochemistry (σ_{PSII}, $Å^2$ $quanta^{-1}$). We previously showed that this broad-band blue-light treatment affects the cells similarly to a high-light treatment with unfiltered fluorescent light (Wu et al., 2011). Samples were collected prior to the onset of high light (plotted as time 0) and after 15, 30, 60, and 90 min for chlorophyll fluorescence analyses and for filtration onto glass fiber filters, which were flash frozen for later protein immunoblotting and pigment analyses. Following the high-light treatment, the remaining culture volumes were returned to their initial growth light of 30 μmol photons m^{-2} s^{-1} for a 30-min recovery period followed by the final sampling.

Fluorescence Measurement and Photoinactivation Parameterization

Chlorophyll fluorescence data were collected using a Xe-PAM fluorometer (Walz) connected to a temperature-controlled cuvette holder (Walz). At each sampling point, a sample of culture was dark adapted for 5 min to relax photosynthetic activity. A modulated (4 Hz) blue-light measuring beam was used to measure F_0, followed by a 500-ms saturating white-light pulse of 4,000 μmol photons m^{-2} s^{-1} to measure F_{Mdark}. Actinic light was then administered with identical conditions to the treatment light (450 μmol blue photons m^{-2} s^{-1}), and F_s, the steady-state fluorescence level in a light-acclimated sample, was measured. Another saturating pulse was then applied to measure maximal fluorescence in the light (F_M'). The maximum quantum yield of PSII photochemistry (van Kooten and Snel, 1990) was then estimated as:

$$F_V/F_M = (F_M - F_0)/F_M$$

Two kinetic phases of NPQ were estimated (Table II). Dynamic NPQ, NPQ_d that relaxed within the 5-min dark period before measurement, and was then reinduced within the short measuring period was estimated as:

$$NPQ_d = (F_M - F_M')/F_M'$$

This NPQ_d phase is equivalent to the NPQ estimated by Zhu and Green (2010) following Bilger and Bjorkman (1990).

A more sustained phase of NPQ, NPQ_s, which was induced over the course of the high-light treatment, and which persisted through the 5-min dark acclimation period just before measurement, was estimated as:

$$NPQ_s = (F_{Mt0} - F_M)/F_M$$

F_{Mt0} is the measurement of F_M from dark-acclimated cells, taken at time 0 just before the start of high-light treatment. F_M is taken at each measurement time point. By definition, NPQ_s thus starts at 0 at T_0, and increases if the cells accumulate a sustained phase of NPQ. Because our repeated time course measurements were conducted rapidly during short-term light-shift experiments to track PSII photoinactivation, we did not apply longer-term relaxation periods (Goss et al., 2006), as used by Zhu and Green (2010) to estimate q_E and q_I according to Farber et al. (1997). NPQ_s reflects an inducible increase in the relaxation time for a fraction of NPQ, persisting beyond a 5-min dark period, but largely relaxing over a 30-min period of low light, even when chloroplastic protein synthesis is blocked. NPQ_s is thus similar to the q_Z defined by Nilkens et al. (2010). Finally, we calculated the total accumulated NPQ_t as the sum of NPQ_d and NPQ_s.

We estimated a functional absorption cross section driving the photoinactivation of PSII (σ_i, Å^2 quanta^{-1}; Campbell and Tyystjärvi, 2012) by plotting a single-phase exponential decay through a plot of F_V/F_M, corrected for any influence of sustained NPQ, versus the cumulative photons (quanta Å^{-2}) applied during the 450 μmol photons m^{-2} s^{-1} light treatment. The correction for sustained NPQ was applied by determining the amplitude of recovery (if any) in F_V/F_M in cells incubated with lincomycin, and transferred from the 450 μmol photons m^{-2} s^{-1} light treatment back down to growth light of 30 μmol photons m^{-2} s^{-1}, for a 30-min recovery period (e.g. Fig. 1A). This recovery amplitude in the presence of lincomycin was attributed to relaxation of sustained NPQ. F_V/F_M values measured during the 450 μmol photons m^{-2} s^{-1} light treatment were corrected upward by this sustained NPQ amplitude, prior to the curve fitting for estimation of σ_i, to separate photoinactivation of PSII from the influence of sustained NPQ. As seen in Figure 1, the amplitudes of the low-light recovery in lincomycin-treated cells are small relative to the declines in F_V/F_M measured during the preceding high-light treatment. The units for σ_i are the same as the units for the functional absorption cross section for PSII photochemistry (σ_{PSII}, Å^2 quanta^{-1}; Falkowski and Raven, 1997); in both cases these are notional areas measuring the probability that an incident photon provokes a given response of photoinactivation or photochemistry. σ_i and σ_{PSII}, are not physical areas of cellular nor molecular structures. Multiplying σ_i by the applied photons Å^{-2} s^{-1} generates a rate constant for photoinactivation, k_{pi}, (s^{-1}; Kok, 1956) for the particular applied light level (Campbell and Tyystjärvi, 2012).

The functional absorption cross section serving PSII photochemistry (σ_{PSII}, Å^2 quanta^{-1}; Falkowski and Raven, 1997; Suggett et al., 2004), was determined on a culture sample dark acclimated for 5 min and then exposed to a saturating single turnover flash (blue LED, 80 μs, 455 ± 20 nm; FIRe fluorometer, Satlantic). σ_{PSII}', the achieved functional absorption cross section in the presence of actinic light was measured by using the actinic light accessory of the FIRe fluorometer to apply 450 μmol photons m^{-2} s^{-1} to the measurement cuvette, followed by application of the saturating single-turnover flash to close all PSII centers. Values of σ_{PSII} were determined from the fluorescence saturation curves analyzed with MATLAB software using the Fireworx program (Barnett, 2007), with instrument-specific light calibration factors (Satlantic).

Validation of F_V/F_M by Oxygen Flash Yield Quantitation of the Content of Active PSII

As a validation and cross check of the rapid, low-sample volume F_V/F_M measures we used to track changes in PSII function during the light-shift experiments presented in Figures 1, 4, and 10, we subsequently conducted a series of measurements on nine different *T. pseudonana* cultures grown at 18°C under 30 ($n = 6$), 90 ($n = 1$), 180 ($n = 1$), or 270 ($n = 1$) μmol photons m^{-2} s^{-1} for multiple rounds of media transfer and many generations of growth. We then shifted the cultures to combinations of 90 ($n = 1$), 180 ($n = 1$), 270 ($n = 1$), 450 ($n = 6$), 1,000 ($n = 2$), 1,400 ($n = 2$), 1,800 ($n = 1$), or 2,200 ($n = 1$) μmol photons m^{-2} s^{-1} for 30 to 90 min, with or without lincomycin.

Before, and after, light-shift treatments we used a modulated fluorometer to measure F_V/F_M from culture samples, as described above. At the same times we took 100-mL culture samples and concentrated them 20× by gentle centrifugation at 4,000*g* and resuspension in 5 mL of the residual growth media supernatant (not fresh media). This concentration step was needed to give sufficient culture density to provoke detectable, short-term, changes in oxygen concentration in the media. We loaded 2.5 mL of the resulting concentrated culture into a plastic 1-cm path length spectrophotometer cuvette and measured the oxygen content of the culture samples using a Foxy R oxygen sensor (Ocean Optics; Bacon and Demas, 1987), mounted in a lab-built epoxy gas-tight cuvette plug that incorporates the oxygen sensor, a temperature probe, and a thermostatted temperature control loop, which we set to 18°C. The entire assembly was then mounted into the SuperHead unit of a PSI FL3500 fluorometer (PSI). This fluorometer unit contains LED light sources that can provide repetitive trains of blue- or red-light flashes of up to 90,000 μmol photons m^{-2} s^{-1} with durations as short as 2 μs. Before any oxygen flash yield experiments were carried out on a given day, the oxygen sensor was calibrated. Distilled water was shaken for 2 min to give air-saturated seawater, at an oxygen content of 238 μmol O_2 L^{-1} (YSI model 51B dissolved oxygen meter instructions, YSI). The oxygen-saturated seawater medium was measured with the oxygen sensor, the reading was allowed to stabilize, and the reading of the oxygen sensor was recorded. The oxygen sensor was then immersed in 2 mol L^{-1} sodium dithionite (Flinn Scientific Inc.), which consumes oxygen, rendering the oxygen content of the solution effectively zero (Jhaveri and Sharma, 1968). The reading was allowed to stabilize and the reading of the oxygen sensor was recorded, to establish the response range of the instrument. After initial stabilization the temperature in the cuvette assembly was maintained within 0.2°C throughout subsequent readings.

Concentrated culture samples were loaded into the cuvette assembly and were then kept in the dark for 3 min while the temperature stabilized. Note that during prior centrifugation and resuspension the cells were in darkness or low light for 20 min prior to oxygen measurements. Once the instrument read the expected steady downward slope in the levels of oxygen in the culture suspensions we used the PSI Superhead system to apply 1 min of low-level (50 μmol photons m^{-2} s^{-1} of combined red and blue light) continuous preillumination, to ensure induction of electron transport through both PSI and PSII during the subsequent flash train (Kuvykin et al., 2008). Following the 1-min preillumination, the oxygen content of the samples was tracked while we used the Superhead to apply a flash train of 3,000 red-light flashes of 20 μs duration, approximately 88,000 μmol photons m^{-2} s^{-1}, spaced by 50-ms dark intervals, giving a flash train lasting 150 s in total. We used multiple test samples to verify that this flash train was indeed sufficient to provide saturating, single-turnover flashes by varying the level, duration, and dark spacing of the flashes. Following the flash train, the sample was kept in the dark once more while oxygen consumption was measured to account for the base rate of cellular respiration that took place during the flash train. We then extracted total chlorophyll from the concentrated culture sample into 90% acetone, measured absorbance, and used the equations of Jeffrey and Humphrey (1975) to estimate the chlorophyll content of the concentrated culture suspensions. We followed the method of Chow et al. (1989) to use the change in oxygen concentration provoked by the series of single-turnover saturating flashes to estimate the content of active PSII per chlorophyll in the suspension as:

$$(\text{mol } O_2\ l^{-1}\ s^{-1}) \times (5\times10^{-2}\ \text{s flash cycle}^{-1}) \times (4\ \text{mol e- 1 mol } O_2^{-1}) \times (1\ \text{flash cycle mol PSII mol e-}^{-1}) \times (1\ \text{L mol Chl}^{-1})$$

In Figure 11 we present the results of this cross validation by plotting F_V/F_M from the cultures treated under high light, with or without lincomycin, as percent of growth level F_V/F_M, versus the content of active PSII in the same cultures, as percent of active PSII in the same culture under growth conditions. The slopes of the linear regressions for measurements with (closed circles) or without (open circles; some data points obscured) lincomycin were not statistically significantly different (*F* test) so we present a pooled linear regression for the combined data from culture samples treated with or without lincomycin. Note the strong correlation between F_V/F_M and the content of active PSII in the cultures. A particular concern of reviewers was that sustained phase(s) of NPQ could suppress F_V/F_M measures, leading to overestimations of the extent of photoinactivation of PSII in our treatments. In fact, Figure 11 shows that as the content of active PSII in the culture declines toward zero under strongly photoinhibitory conditions, there is a *y* intercept of F_V/F_M of 33% of control levels of F_V/F_M. Therefore, in strongly photoinhibited cultures the F_V/F_M measure we used somewhat underestimates the loss of PSII activity, rather than overestimating the loss of activity. We are thus confident that our estimates of rate constants for photoinactivation (Fig. 4) are conservative, rather than exaggerated, and that photoinactivation rate constants can indeed exceed rate constants for clearance of PsbA (Figs. 2 and 4), as reviewed by Edelman and Mattoo (2008).

Quantitation of Proteins by Immunoblotting

Cells were harvested on glass fiber filters (0.7-μm effective pore size, 25-mm diameter, binder-free glass fiber, Whatman), which were immediately flash frozen in liquid nitrogen and stored at −80°C for later protein analyses. We quantified molar levels of PsbA and PsbD from samples taken during the high-light treatment time courses. Total proteins were extracted by two thawing/sonicating rounds in denaturing extraction buffer (Brown et al., 2008). The total protein concentration was determined (Lowry protein assay kit, BioRad-DC Assay). One microgram of total protein was loaded on 4% to 12% acrylamide precast NuPAGE gels (Invitrogen) for determination of PsbA and PsbD, run in parallel with a range of protein quantitation standards for each target protein (Agrisera, www.agrisera.se) to establish a standard curve. Electrophoresis was run for 40 min at 200 V and the proteins were transferred to a polyvinylidene difluoride membrane. After membrane blocking, primary antibody against the C-terminal part of PsbA (Agrisera, 1:50,000) or the N-terminal region of PsbD (AgriSera, 1:50,000) were applied, followed by an anti-rabbit secondary antibody coupled with horseradish peroxidase. The membranes were developed by chemoluminescence using ECL Advance (Amersham biosciences) and a CCD imager (BioRad VersaDoc 4000MP). PsbA and PsbD protein contents were determined by fitting the sample signal values to the protein standard curves, taking care that all sample signals fell within the range of the protein standard curve, and that no band signals were saturated. We estimated a rate constant for the clearance of PsbA protein by plotting fmol PsbA μg total protein^{-1}, for cells incubated under the 450 μmol photons m^{-2} s^{-1} treatment in the presence of lincomycin to block the counteracting synthesis of PsbA through chloroplast translation. We fit this PsbA plot with a single-phase exponential decay over the period from 15 to 90 min of high-light incubation, to account for any initial induction period of PsbA removal immediately after the upward light shift. This k_{psbA} rate constant expresses the loss of PsbA protein relative to the total pool of PsbA protein. In fact, mechanistically, the clearance of PsbA protein from the thylakoid membranes is believed to act upon photoinactivated PSII centers (Nixon et al., 2010), not upon the total pool of PsbA that is found in both $[PSII]_{active}$ + $[PSII]_{inactive}$. Therefore, the k_{psbA} rate constant for removal of PsbA is not directly applicable to a mechanistic model of the PSII repair cycle, but k_{psbA} does reflect the capacity for removal of PsbA protein from the PSII pool.

Similar methods were used to detect relative changes in levels of Lhcx1 and Lhcx6 proteins between control cells taken before the high-light treatment, and cells taken after 90 min of high-light treatment. Total protein extracts containing 0.06 μg chlorophyll *a* were loaded per lane (approximately 3 μg of total protein) and ECL and autoradiography film were used for detection. The anti-Lhcx1 antibody was the generous gift of Dr. Erhard Rhiel; the anti-Lhcx6 antibody was prepared by Agrisera (Zhu and Green, 2010). Changes in Lhcx1 and Lhcx6 were quantified by digitizing the autoradiography signals using the same BioRad VersaDoc 4000MP imager and then normalizing the target protein signals to the signal from the 20-kD band of MagicMark XP markers (Invitrogen) run on each gel, taking care that the band densities for quantitation remained below the saturation limit of the autoradiography film.

Pigment Analyses

A 20-mL volume of each culture replicate was filtered onto 25-mm-diameter Whatman GF/F glass fiber filters. Filters were immediately flash frozen in liquid nitrogen and stored at −80°C until analysis. Pigments were extracted from the filter in 95% methanol and sonicated on ice (Sonicator Ultrasonic Processor XL 2010). The extracts were cleared from any filter debris by centrifugation and filtration through a 0.22-μm PTFE syringe filter and then separated using HPLC (Zapata et al., 2000). Pigments were identified according to their retention time and spectrum, and quantified by comparison with standards (DHI, http://c14.dhigroup.com). Transβ-Apo-8′-carotenal was used as an internal standard.

Curve Fitting and Statistical Analyses

We used Prism 5.0 (www.graphpad.com) for curve fitting and statistical comparisons.

ACKNOWLEDGMENTS

The authors thank two anonymous reviewers whose detailed comments helped improve the manuscript. We thank Paul Shaver for assistance commissioning the oxygen flash yield system.

Received July 3, 2012; accepted July 23, 2012; published July 24, 2012.

LITERATURE CITED

Anderson NJ (2000) Miniview: diatoms, temperature and climatic change. Eur J Phycol **35:** 307–314

Aro EM, Suorsa M, Rokka A, Allahverdiyeva Y, Paakkarinen V, Saleem A, Battchikova N, Rintamäki E (2005) Dynamics of photosystem II: a proteomic approach to thylakoid protein complexes. J Exp Bot **56:** 347–356

Aro EM, Virgin I, Andersson B (1993) Photoinhibition of photosystem II: inactivation, protein damage and turnover. Biochim Biophys Acta **1143:** 113–134

Bachmann KM, Ebbert V, Adams WW, Verhoeven AS, Logan BA, Demmig-Adams B (2004) Effects of lincomycin on PSII efficiency, non-photochemical quenching, D1 protein and xanthophyll cycle during photoinhibition and recovery. Funct Plant Biol **31:** 803–813

Bacon JR, Demas JN (1987) Determination of oxygen concentrations by luminescence quenching of a polymer-immobilized transition-metal complex. Anal Chem **59:** 2780–2785

Bailleul B, Rogato A, de Martino A, Coesel S, Cardol P, Bowler C, Falciatore A, Finazzi G (2010) An atypical member of the light-harvesting complex stress-related protein family modulates diatom responses to light. Proc Natl Acad Sci USA **107:** 18214–18219

Barnett AB (2007) Fireworx 1.0.3. Dalhousie University: Halifax, NS, Canada. http://sourceforge.net/projects/fireworx (May 16, 2011)

Baroli I, Melis A (1996) Photoinhibition and repair in *Dunaliella salina* acclimated to different growth irradiances. Planta **198:** 640–646

Bilger W, Bjorkman O (1990) Role of the xanthophyll cycle in photoprotection elucidated by measurements of light-induced absorbency changes, fluorescence and photosynthesis in leaves of *Hedera canariensis*. Photosynth Res **25:** 173–185

Brown CM, MacKinnon JD, Cockshutt AM, Villareal T, Campbell DA (2008) Flux capacities and acclimation costs in *Trichodesmium* from the Gulf of Mexico. Mar Biol **154:** 413–422

Campbell DA, Tyystjärvi E (2012) Parameterization of photosystem II photoinactivation and repair. Biochim Biophys Acta **1817:** 258–265

Chow WS, Hope AB, Anderson JM (1989) Oxygen per flash from leaf disks quantifies photosystem II. Biochim Biophys Acta **973:** 105–108

Depauw FA, Rogato A, Ribera d'Alcalá M, Falciatore A (2012) Exploring the molecular basis of responses to light in marine diatoms. J Exp Bot **63:** 1575–1591

Dimier C, Corato F, Tramontano F, Brunet C (2007) Photoprotective capacity as functional trait in planktonic algae: relationship between xanthophyll cycle and ecological characteristics in three diatoms. J Phycol **43:** 937–947

Dubinsky Z, Stambler N (2009) Photoacclimation processes in phytoplankton: mechanisms, consequences, and applications. Aquat Microb Ecol **56:** 163–176

Edelman M, Mattoo AK (2008) D1-protein dynamics in photosystem II: the lingering enigma. Photosynth Res **98:** 609–620

Eisenstadt D, Barkan E, Luz B, Kaplan A (2010) Enrichment of oxygen heavy isotopes during photosynthesis in phytoplankton. Photosynth Res **103:** 97–103

Eisenstadt D, Ohad I, Keren N, Kaplan A (2008) Changes in the photosynthetic reaction centre II in the diatom *Phaeodactylum tricornutum* result in non-photochemical fluorescence quenching. Environ Microbiol **10:** 1997–2007

Falkowski P, Raven JA (2007) Aquatic Photosynthesis, Ed 2. Blackwell Science, Oxford, pp 102–117

Falkowski PG, Owens TG (1980) Light shade adaptation: two strategies in marine phytoplankton. Plant Physiol **66:** 592–595

Farber A, Young AJ, Ruban AV, Horton P, Jahns P (1997) Dynamics of xanthophyll-cycle activity in different antenna subcomplexes in the photosynthetic membranes of higher plants (The relationship between zeaxanthin conversion and nonphotochemical fluorescence quenching). Plant Physiol **115:** 1609–1618

Field CB, Behrenfeld MJ, Randerson JT, Falkowski PG (1998) Primary production of the biosphere: integrating terrestrial and oceanic components. Science **281:** 237–240

Finkel ZV (2001) Light absorption and size scaling of light limited metabolism in marine diatoms. Limnol Oceanogr **46:** 86–94

Goericke R, Welschmeyer NA (1992) Pigment turnover in the marine diatom *Thalassiosira weissflogii*. II. The $^{14}CO_2$-labeling kinetics of carotenoids. J Phycol **25:** 507–517

Goss R, Ann Pinto E, Wilhelm C, Richter M (2006) The importance of a highly active and DeltapH-regulated diatoxanthin epoxidase for the

regulation of the PS II antenna function in diadinoxanthin cycle containing algae. J Plant Physiol **163:** 1008–1021

Goss R, Jakob T (2010) Regulation and function of xanthophyll cycle-dependent photoprotection in algae. Photosynth Res **106:** 103–122

Grouneva I, Jakob T, Wilhelm C, Goss R (2008) A new multicomponent NPQ mechanism in the diatom Cyclotella meneghiniana. Plant Cell Physiol **49:** 1217–1225

Grouneva I, Jakob T, Wilhelm C, Goss R (2009) The regulation of xanthophyll cycle activity and of non-photochemical fluorescence quenching by two alternative electron flows in the diatoms *Phaeodactylum tricornutum* and *Cyclotella meneghiniana.* Biochim Biophys Acta **1787:** 929–938

Houghton JT, Ding Y, Griggs DJ, Noguer M, Van der Linden PJ, Dai X, Maskell K, Johnson CA (2001) Climate Change 2001: The Scientific Basis. Cambridge University Press, Cambridge, UK, pp 881

Huner NPA, Öquist G, Sarhan F (1998) Energy balance and acclimation to light and cold. Trends Plant Sci **3:** 224–230

Janknegt P, de Graaff M, van de Poll W, Visser R, Rijstenbil J, Buma A (2009) Short term antioxidative responses of 15 microalgae exposed to excessive irradiance including ultraviolet radiation. Eur J Phycol **44:** 525–539

Jeffrey SW, Humphrey GF (1975) New spectrophotometric equations for determining chlorophylls a, b, c1 and c2 in higher plants, algae, and natural phytoplankton. Biochem Physiol Pflanz **167:** 191–194

Jhaveri AS, Sharma MM (1968) Absorption of oxygen in aqueous alkaline solutions of sodium dithionite. Chem Eng Sci **23:** 1–8

Keller MD, Selvin RC, Claus W, Guillard RRL (1987) Media for the culture of oceanic ultraphytoplankton. J Phycol **23:** 633–638

Key T, McCarthy A, Campbell DA, Six C, Roy S, Finkel ZV (2010) Cell size trade-offs govern light exploitation strategies in marine phytoplankton. Environ Microbiol **12:** 95–104

Kok B (1956) On the inhibition of photosynthesis by intense light. Biochim Biophys Acta **21:** 234–244

Komenda J, Sobotka R, Nixon PJ (2012) Assembling and maintaining the photosystem II complex in chloroplasts and cyanobacteria. Curr Opin Plant Biol **15:** 245–251

Kuvykin IV, Vershubskii AV, Ptushenko VV, Tikhonov AN (2008) Oxygen as an alternative electron acceptor in the photosynthetic electron transport chain of C3 plants. Biochemistry (Mosc) **73:** 1063–1075

Lavaud J (2007) Fast regulation of photosynthesis in diatoms: mechanisms, evolution and ecophysiology. Func Plant Sci Biotech **1:** 267–287

Lavaud J, Kroth PG (2006) In diatoms, the transthylakoid proton gradient regulates the photoprotective non-photochemical fluorescence quenching beyond its control on the xanthophyll cycle. Plant Cell Physiol **47:** 1010–1016

Lavaud J, Rousseau B, Etienne A-L (2002a) In diatoms, a transthylakoid proton gradient alone is not sufficient to induce a non-photochemical fluorescence quenching. FEBS Lett **523:** 163–166

Lavaud J, Rousseau B, Etienne A-L (2004) General features of photoprotection by energy dissipation in planktonic diatoms (Bacillariophyceae). J Phycol **40:** 130–137

Lavaud J, Rousseau B, van Gorkom HJ, Etienne A-L (2002b) Influence of the diadinoxanthin pool size on photoprotection in the marine planktonic diatom *Phaeodactylum tricornutum.* Plant Physiol **129:** 1398–1406

Lavaud J, Strzepek RF, Kroth PG (2007) Photoprotection capacity differs among diatoms: possible consequence on the spatial distribution of diatoms related to fluctuations in the underwater light climate. Limnol Oceanogr **52:** 1188–1194

Lepetit B, Goss R, Jakob T, Wilhelm C (2012) Molecular dynamics of the diatom thylakoid membrane under different light conditions. Photosynth Res **111:** 245–257

Lepetit B, Volke D, Gilbert M, Wilhelm C, Goss R (2010) Evidence for the existence of one antenna-associated, lipid-dissolved and two protein-bound pools of diadinoxanthin cycle pigments in diatoms. Plant Physiol **154:** 1905–1920

Lohr M, Wilhelm C (1999) Algae displaying the diadinoxanthin cycle also possess the violaxanthin cycle. Proc Natl Acad Sci USA **96:** 8784–8789

Lohr M, Wilhelm C (2001) Xanthophyll synthesis in diatoms: quantification of putative intermediates and comparison of pigment conversion kinetics with rate constants derived from a model. Planta **212:** 382–391

Long SP, Humphries S, Falkowski PG (1994) Photoinhibition of photosynthesis in nature. Annu Rev Plant Physiol Plant Mol Biol **45:** 633–662

Mauzerall D (1982) Statistical theory of the effect of multiple excitations in photosynthetic systems. *In* RR Alfano, eds, Biological Events Probed by Ultrafast Laser Spectroscopy. Academic Press, New York, pp 215–235

Morel A, Bricaud A (1981) Theoretical results concerning light absorption in a discrete medium, and application to specific absorption of phytoplankton. Deep-Sea Res **28A:** 1375–1393

Müller P, Li X-P, Niyogi KK (2001) Non-photochemical quenching: a response to excess light energy. Plant Physiol **125:** 1558–1566

Murata N, Takahashi S, Nishiyama Y, Allakhverdiev SI (2007) Photoinhibition of photosystem II under environmental stress. Biochim Biophys Acta **1767:** 414–421

Nilkens M, Kress E, Lambrev P, Miloslavina Y, Müller M, Holzwarth AR, Jahns P (2010) Identification of a slowly inducible zeaxanthin-dependent component of non-photochemical quenching of chlorophyll fluorescence generated under steady-state conditions in *Arabidopsis.* Biochim Biophys Acta **1797:** 466–475

Nishiyama Y, Allakhverdiev SI, Murata N (2005) Inhibition of the repair of photosystem II by oxidative stress in cyanobacteria. Photosynth Res **84:** 1–7

Nishiyama Y, Allakhverdiev SI, Murata N (2006) A new paradigm for the action of reactive oxygen species in the photoinhibition of photosystem II. Biochim Biophys Acta **1757:** 742–749

Nixon PJ, Michoux F, Yu J, Boehm M, Komenda J (2010) Recent advances in understanding the assembly and repair of photosystem II. Ann Bot (Lond) **106:** 1–16

Pascal AA, Caron L, Rousseau B, Lapouge K, Duval JC, Robert B (1998) Resonance Raman spectroscopy of a light-harvesting protein from the brown alga *Laminaria saccharina.* Biochemistry **37:** 2450–2457

Raven JA (2011) The cost of photoinhibition. Physiol Plant **142:** 87–104

Schumann A, Goss R, Torsten J, Wilhelm C (2007) Investigation of the quenching efficiency of diatoxanthin in cells of *Phaeodactylum tricornutum* (Bacillariophyceae) with different pool sizes of xanthophyll cycle pigments. Phycologia **46:** 113–117

Silva P, Thompson E, Bailey S, Kruse O, Mullineaux CW, Robinson C, Mann NH, Nixon PJ (2003) FtsH is involved in the early stages of repair of photosystem II in *Synechocystis* sp PCC 6803. Plant Cell **15:** 2152–2164

Six C, Finkel ZV, Irwin AJ, Campbell DA (2007) Light variability illuminates niche-partitioning among marine Picocyanobacteria. PLoS ONE **2:** e1341

Six C, Sherrard R, Lionard M, Roy S, Campbell DA (2009) Photosystem II and pigment dynamics among ecotypes of the green alga *Ostreococcus.* Plant Physiol **151:** 379–390

Strzepek RF, Harrison PJ (2004) Photosynthetic architecture differs in coastal and oceanic diatoms. Nature **431:** 689–692

Suggett DJ, MacIntyre HL, Geider RJ (2004) Evaluation of biophysical and optical determinations of light absorption by photosystem II in phytoplankton. Limnol Oceanogr Methods **2:** 316–332

Tyystjärvi E, Aro EM (1996) The rate constant of photoinhibition, measured in lincomycin-treated leaves, is directly proportional to light intensity. Proc Natl Acad Sci USA **93:** 2213–2218

van Kooten O, Snel JFH (1990) The use of chlorophyll fluorescence nomenclature in plant stress physiology. Photosynth Res **25:** 147–150

Waring J, Klenell M, Bechtold U, Underwood GJC, Baker NR (2010) Light-induced responses of oxygen photoreduction, reactive oxygen species production and scavenging in two diatom species. J Phycol **46:** 1206–1217

Wu HY, Cockshutt AM, McCarthy A, Campbell DA (2011) Distinctive photosystem II photoinactivation and protein dynamics in marine diatoms. Plant Physiol **156:** 2184–2195

Zapata M, Rodriguez F, Garrido JL (2000) Separation of chlorophylls and carotenoids from marine phytoplankton: a new HPLC method using a reversed phase C-8 column and pyridine-containing mobile phases. Mar Ecol Prog Ser **195:** 29–45

Zhu SH, Green BR (2010) Photoprotection in the diatom *Thalassiosira pseudonana*: role of LI818-like proteins in response to high light stress. Biochim Biophys Acta **1797:** 1449–1457